Design of High Energy Absorbing Materials Based on Porous Superelastic NiTi

Ying Zhao, Graduate Student
Minoru Taya, Professor and Director

Center for Intelligent Materials and Systems
Department of Mechanical Engineering
University of Washington, Box 352600
Phone: 206-685-2850, Fax: 206-685-8047
email: tayam@u.washington.edu

Applications of porous shape memory alloys (SMAs)

- High energy absorbing Structure and damping devices
- Medical implant
- Cooling surface

Background

(A) Shape memory alloys such as NiTi exhibit larger buckling load as compared with other structural materials (for example aluminum) (Suzuki, Urushiyama and Taya, 2004)

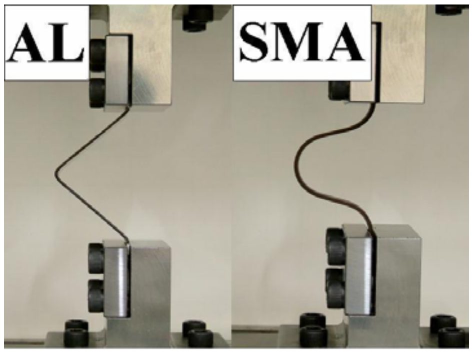

Test specimens after buckling

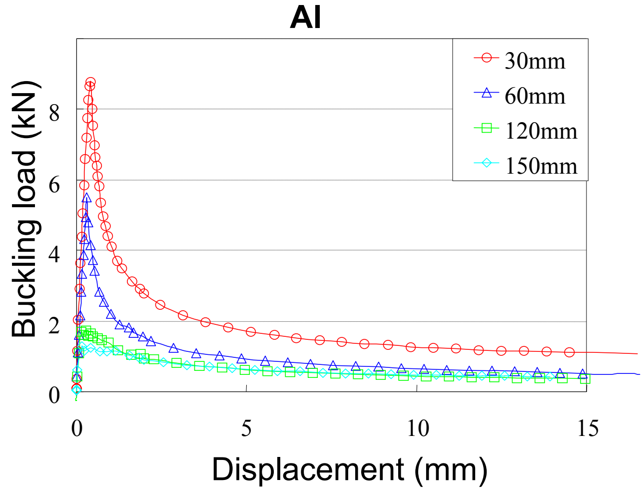

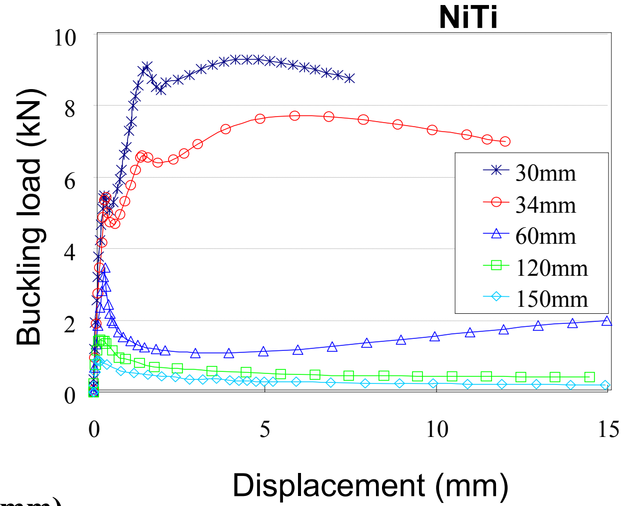

(B) Increase in buckling load by applying side constraint

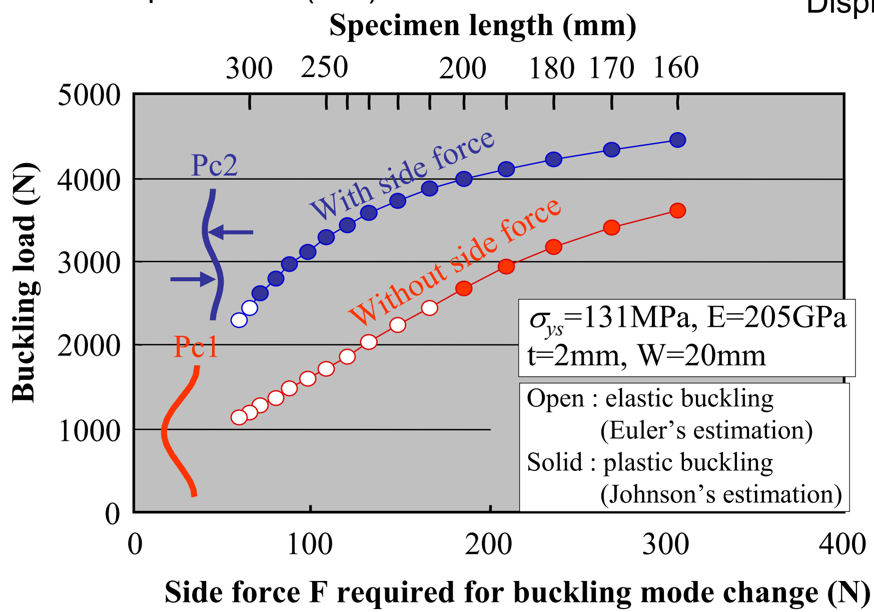

Approach to Design Porous SMA

(1) Combine previous results of (A) and (B) in Background, to design a porous SMA such as NiTi which exhibits large energy absorption capacity per weight.

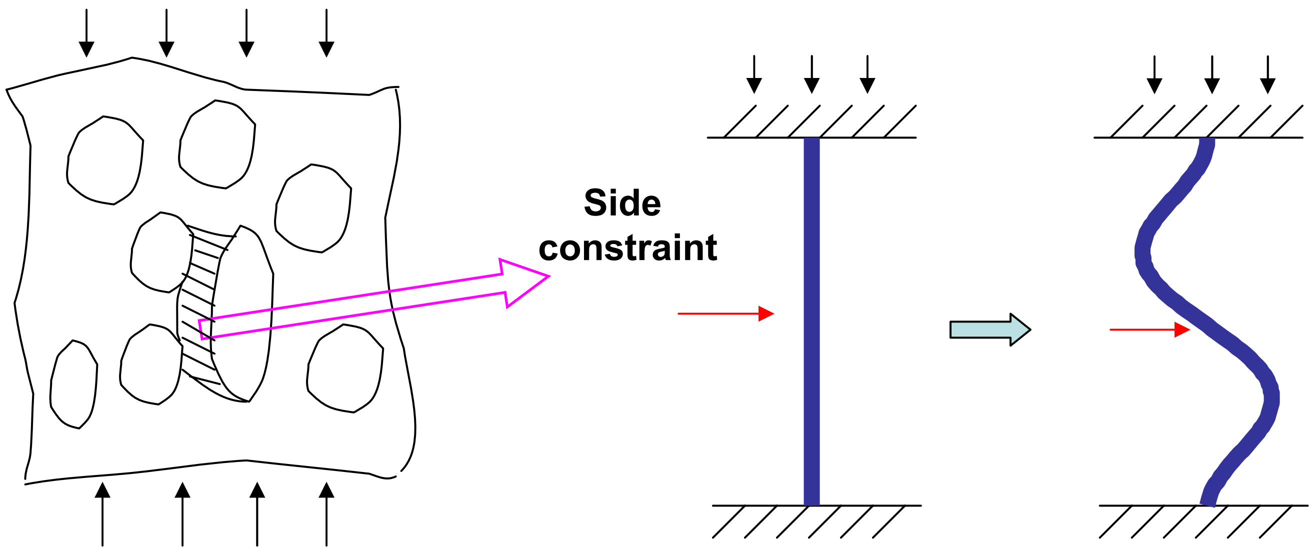

Micro-pillar with side constraint

(2) Use the large stress-strain characteristics of SMA.

(3) Design composite structure made of porous NiTi and NiTi spring

Porous NiTi SMA fabricated by Spark Plasma Sintering (SPS)

Specimen	Porosity (%)	Spark Plasma Processing Condition	Transformation temperature (° C)
Solid NiTi	0	950°C under 50MPa, 5 minutes	A_s = 18.888 A_f = 37.182
13% porous NiTi	13	800°C under 25MPa, 5 minutes	A_s = 1.288 A_f = 23.823

SPS equipment

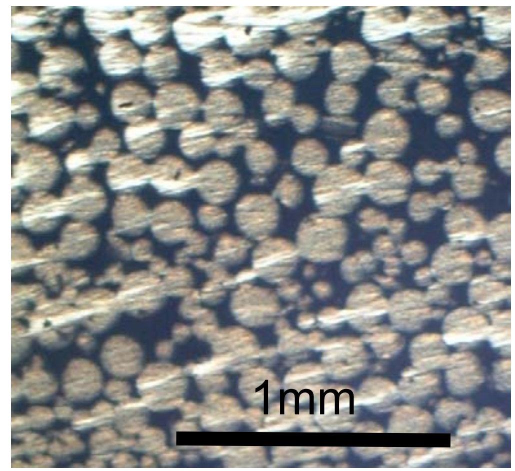

Uniform microstructure of 13% porosity NiTi

Compression tests under room temperature

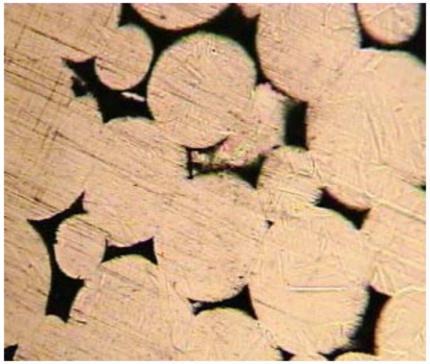

(a) Before Compression

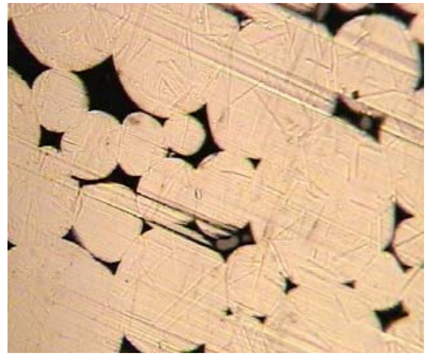

(b) Compression up to 5% and unloaded

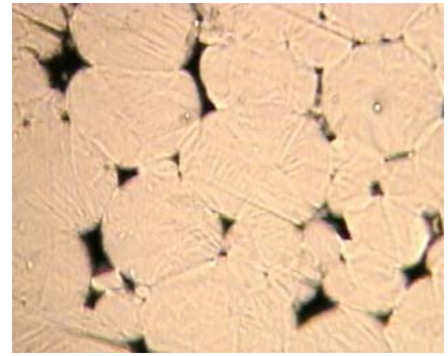

(c) Compression up to 7% and unloaded

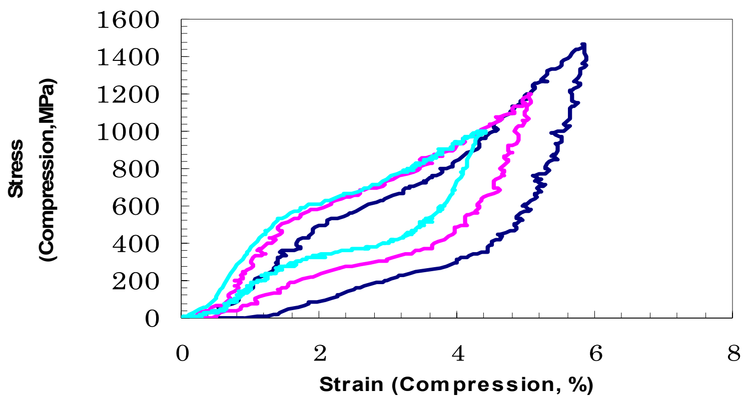

Superelastic response of solid NiTi under static compression

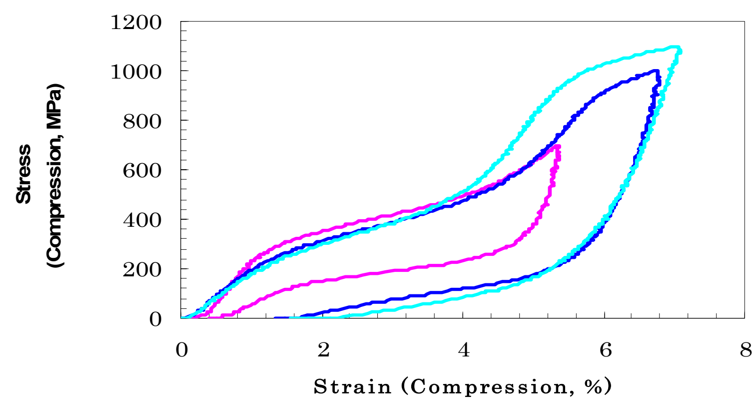

Superelastic response of porous NiTi under static compression (f_p=13%)

Idealized Stress-Strain Curve

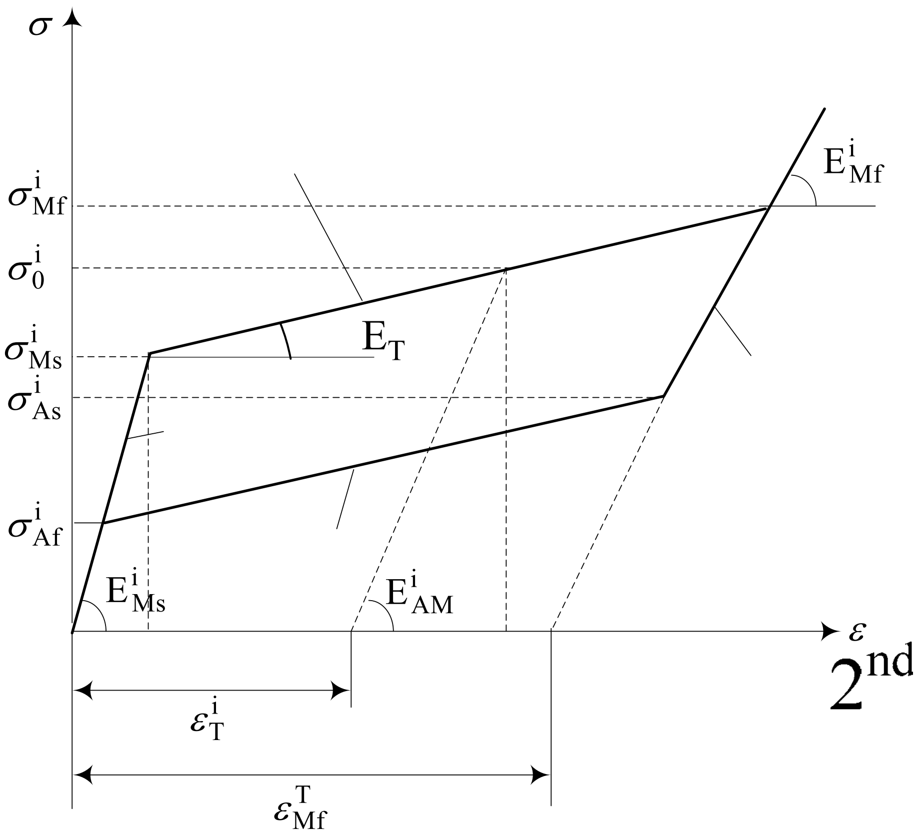

1^{st} Stage

100% austenite, E_{Ms}

2^{nd} Stage

Austenite 100% $\rightarrow$ 0%

Martensite 0% $\rightarrow$ 100%

3^{rd} Stage

100% martensite, E_{Mf}

2^{nd} stage

4^{th} Stage

Austenite 0% $\rightarrow$ 100%

Martensite 100% $\rightarrow$ 0%

C_i

I

B_i

Model-1: Stress-strain curve of NiTi with closed pores

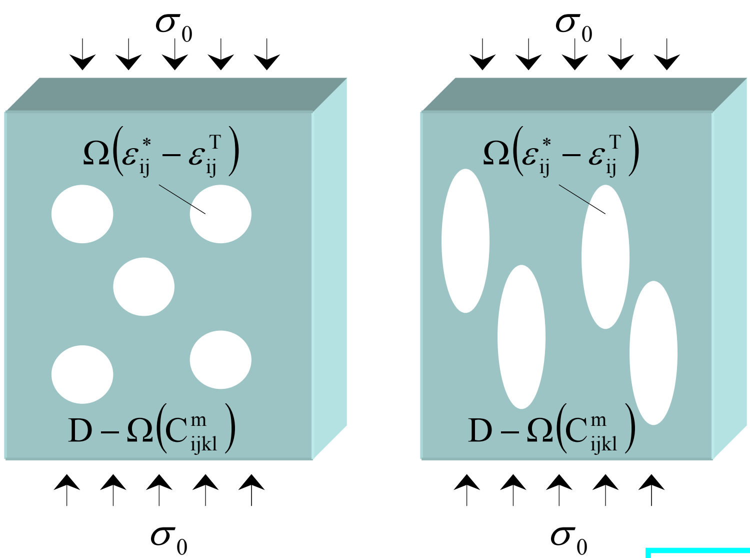

Eshelby's equivalent inclusion method

$$\sigma^0_{ij} + \sigma_{ij} = \mathbf{C}^m_{ijkl}\left[e^0_{kl} + \bar{e}_{kl} + e_{kl} - \left(\varepsilon^*_{kl} - \varepsilon^T_{kl}\right)\right]$$

$$= \mathbf{C}^m_{ijkl}\left(\varepsilon^0_{kl} + \bar{\varepsilon}_{kl} + \varepsilon_{kl} - \varepsilon^{**}_{kl}\right)$$

$$= \mathbf{C}^p_{ijkl}\left(\varepsilon^0_{kl} + \bar{\varepsilon}_{kl} + \varepsilon_{kl}\right)$$

$$\sigma^0_{ij} = \mathbf{C}^m_{ijkl}\varepsilon^0_{kl} \qquad \varepsilon_{kl} = \mathbf{S}_{klmn}\varepsilon^{**}_{mn}$$

$$\varepsilon^{**}_{kl} = -\frac{1}{1-f_p}\left(\mathbf{S}_{klmn} - \mathbf{I}\right)^{-1} C^{m-1}_{ijkl}\sigma^0_{ij}$$

Eigenstrain ε^*_{ij}

Equivalency of total potential energy and work done by σ_0

ε^T_{ij}

E^T

E^P_{Ms} E^P_{Mf}

σ^P_{Ms} σ^P_{Mf} σ^P_{As} σ^P_{Af}

Stress-strain curve

Model-1: Stress-strain curve of NiTi with closed pores

Critical stresses

Bi: $\sigma^{P}_{Ms} = (1-f_P)\sigma^{S}_{Ms}$

Di: $\sigma^{P}_{Mf} = (1-f_P)\sigma^{S}_{Mf}$

di: $\sigma^{P}_{As} = (1-f_p)\sigma^{S}_{As}$

bi: $\sigma^{P}_{Af} = (1-f_p)\sigma^{S}_{Af}$

Linear stage (equivalency of strain energy density)

$$\frac{1}{2}\mathbf{C}^{c-1}_{ijkl}\sigma^{0}_{ij}\sigma^{0}_{kl} = \frac{1}{2}\mathbf{C}^{m-1}_{ijkl}\sigma^{0}_{ij}\sigma^{0}_{kl} + \frac{1}{2}f_P\sigma^{0}_{ij}\varepsilon^{**}_{kl}$$

Stiffness

1st stage

$$\frac{E_{Ms}}{E_A} = \frac{1}{1+\eta f_P}$$

3rd stage

$$\frac{E_{Mf}}{E_M} = \frac{1}{1+\eta f_P}$$

(where $\eta = -\frac{1}{1-f_P}(S_{3333}-1)^{-1}$)

Model-1: Stress-strain curve of NiTi with closed pores

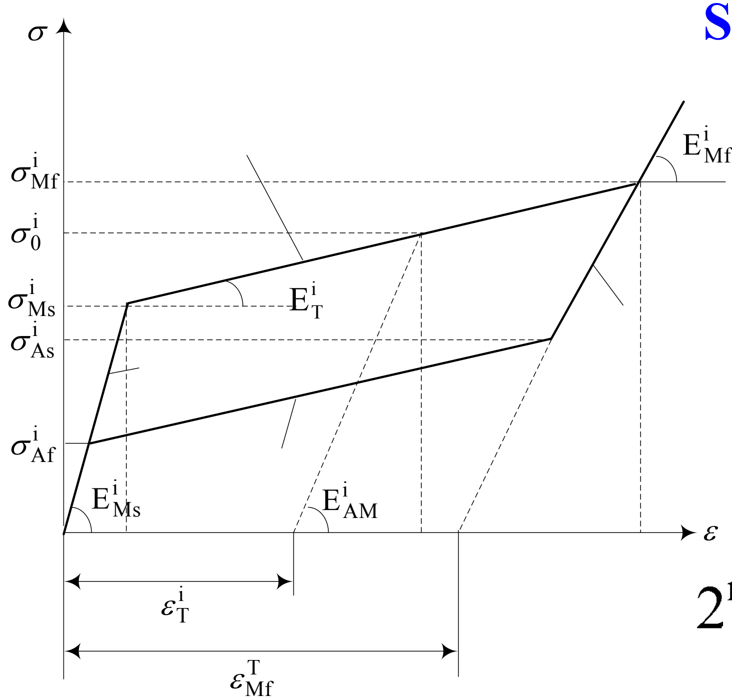

Stress-induced martensitic transformation

Macroscopic strain energy density of porous NiTi

$$W_{macr} = \frac{1}{2}\left(\sigma^{P}_{Ms} + \sigma^{P}_{0}\right)\left(\varepsilon_T + \frac{\sigma^{P}_{0}}{E_{AM}} - \frac{\sigma^{P}_{Ms}}{E_{Ms}}\right)$$

Microscopic stain energy density (Taya et al, 1991)

$$W_{micro} = \frac{1}{2}\mathbf{C}^{m-1}_{ijkl}\sigma^{0}_{ij}\sigma^{0}_{kl} + \frac{1}{2}f_P\sigma^{0}_{ij}\varepsilon^{*}_{kl}(\varepsilon_T)$$

2^{nd} stage

Equating the above two equations given as

$$A\varepsilon_T^2 + B\varepsilon_T + C = 0 \longrightarrow \boxed{\varepsilon_T = \frac{-B + \sqrt{B^2 - 4AC}}{2A}}$$

D_i

C_i

Young's modulus

$$\boxed{E_T = \frac{\sigma^{P}_{0} - \sigma^{P}_{Ms}}{\varepsilon_T}}$$

(2^{nd} and 4^{th} Stage)

d_i 3^{rd} stage

Assume the Young's modulus as the function of transformation strain

$$E^{i}_{AM} = E^{i}_{Ms} - \frac{E^{i}_{Ms} - E^{i}_{Mf}}{\varepsilon^{i}_{Mf} - \sigma^{i}_{Mf}/E^{i}_{Mf}}\varepsilon^{i}_{T}$$

B_i

1^{st} stage

b

Model-2: Stress-strain curve of NiTi with open pores

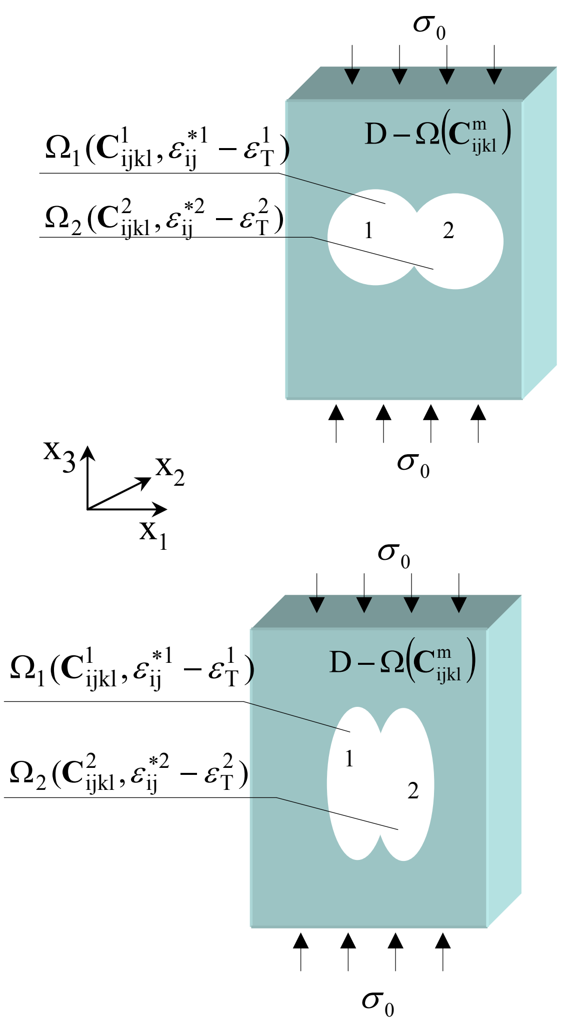

Disturbance stress σ^{1}_{ij}

Disturbance stress σ^{2}_{ij}

Eigenstrain ε^{*1}_{ij} in Ω_1

Eigenstrain ε^{*2}_{ij} in Ω_2

Equivalency of total potential energy and work done by σ_0

Average eigenstrain ε^{*}_{ij}

ε^{T}_{ij}

σ^{P}_{Ms} σ^{P}_{Mf} σ^{P}_{As} σ^{P}_{Af}

E^{P}_{Ms} E^{P}_{Mf}

E^{T}

Model-2: Stress-strain curve of NiTi with open pores

Ratio of Eigenstrain in Ω_2 to Ω_1

$$\varepsilon_{33}^{*2} = \xi \varepsilon_{33}^{*1}$$

$$\xi = -\frac{(1+\nu)(1-2\nu)}{(1-\nu)^2(\mathbf{S}_{3333}-1)}$$

Average eigenstrain

$$\varepsilon_{33}^{*(I/III)} = \frac{1}{2}(1+\xi)\varepsilon_{33}^{*1}$$

$$\varepsilon_{33}^{*(II/IV)} = \frac{1}{2}\left(\varepsilon_T^1 + \varepsilon_T^2\right) - \frac{1}{2}(1+\xi)\varepsilon_{33}^{*1}$$

Transformation strain

$$\varepsilon_T = \frac{-B_2 + \sqrt{(B_2)^2 - 4A_2C_2}}{2A_2}$$

Stiffness

1st stage
$$\frac{E_{Ms}}{E_A} = \frac{1}{1+\eta f_P}$$

2st stage and 4th Stage
$$E_T = \frac{\sigma_0^P - \sigma_{Ms}^P}{\varepsilon_T}$$

3st stage
$$\frac{E_{Mf}}{E_M} = \frac{1}{1+\eta f_P}$$

Critical stress

$$\sigma_{Ms}^P = (1-f_P)\sigma_{Ms}^S \qquad \sigma_{Mf}^P = (1-f_P)\sigma_{Mf}^S$$

$$\sigma_{As}^P = (1-f_p)\sigma_{As}^S \qquad \sigma_{Af}^P = (1-f_p)\sigma_{Af}^S$$

Comparison

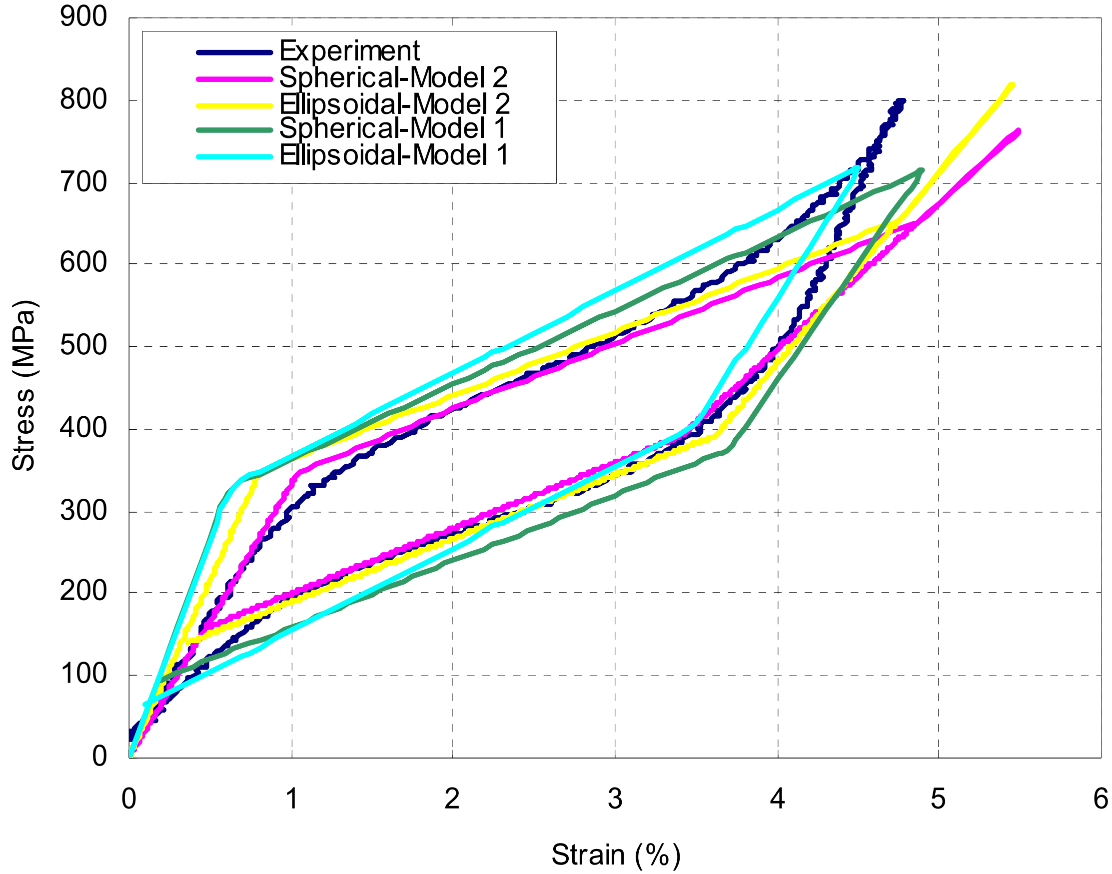

Experiment
Spherical-Model 2
Ellipsoidal-Model 2
Spherical-Model 1
Ellipsoidal-Model 1
Stress (MPa)
0
100
200
300
400
500
600
700
800
900
Strain (%)
0
1
2
3
4
5
6

Composite Design : Porous NiTi Cylinder and NiTi Spring

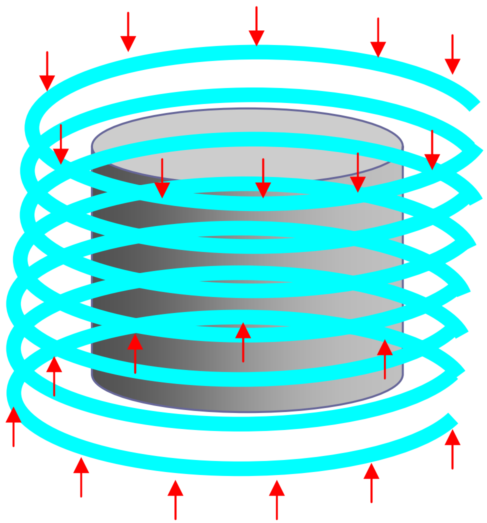

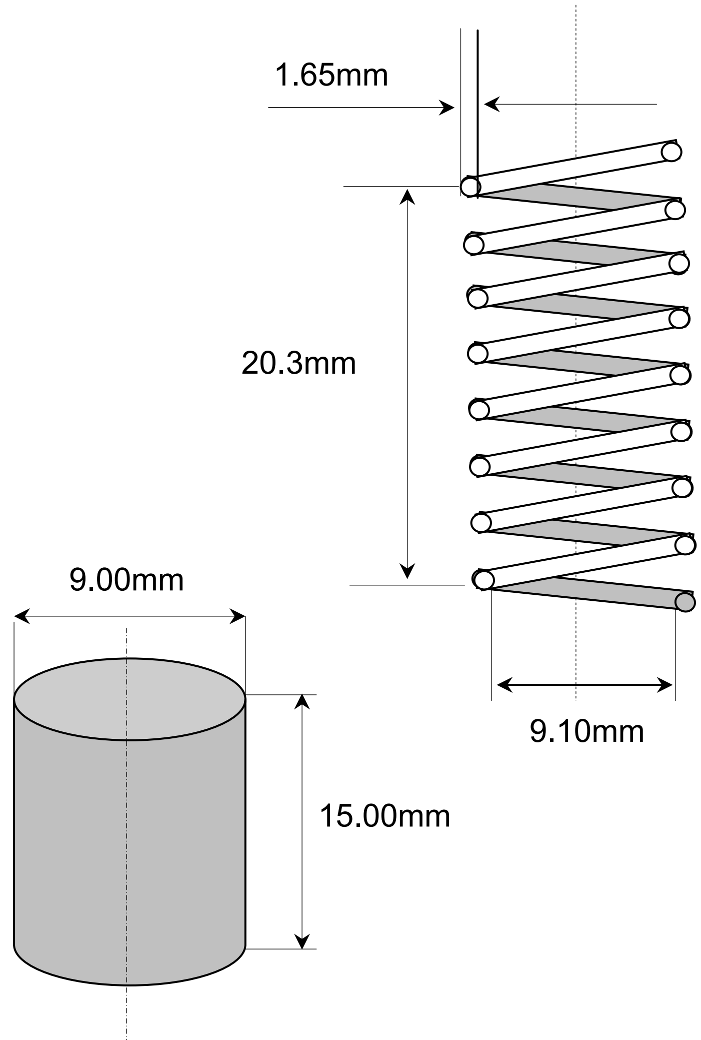

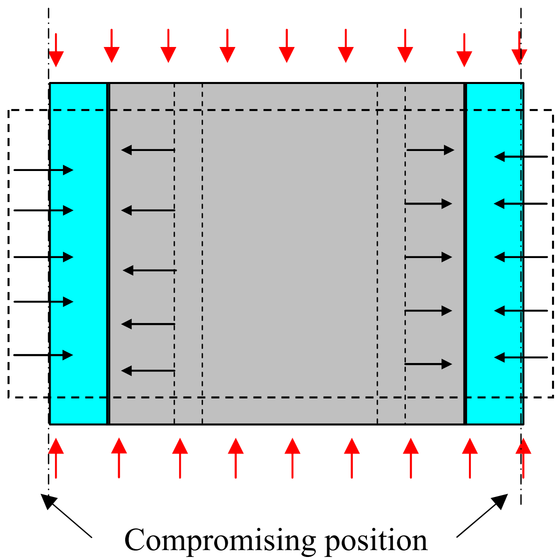

Experimental Results of Composite Design

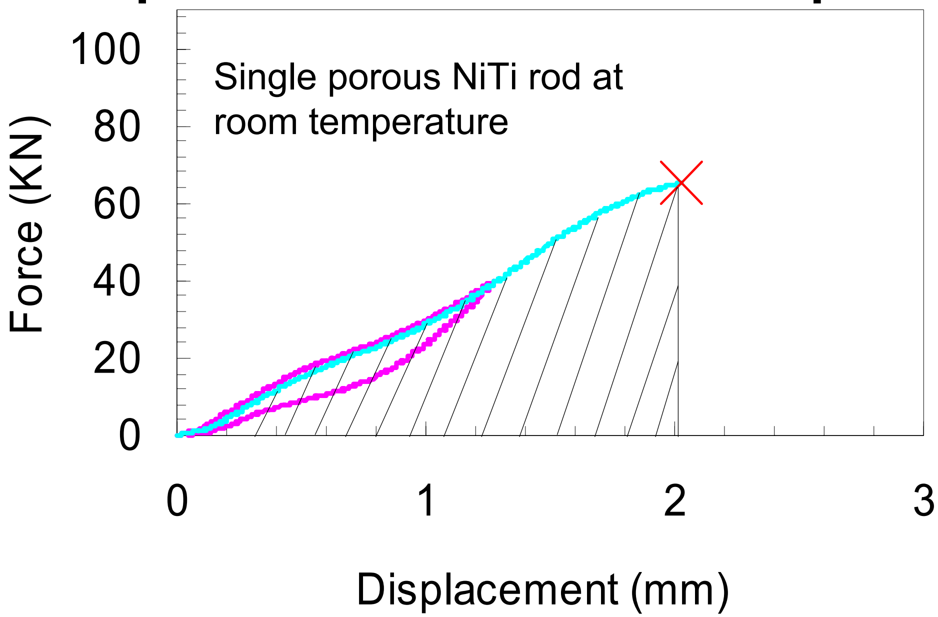

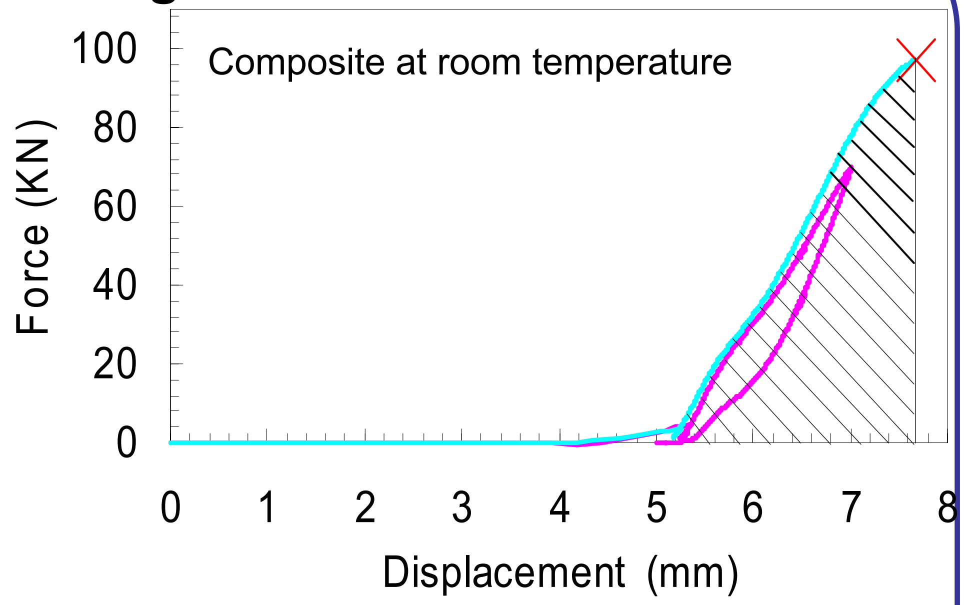

	Maximum Reversible Disp. (mm)	Maximum Reversible Force (KN)	Fracture Disp. (mm)	Fracture Force (KN)	Energy Absorption (EA, J)	Specific EA (J/g)
Single Porous NiTi Rod	1.29 mm	40.74 KN	2.03 mm	65.15 KN	65.1J	12.2 J/g
Composite Structure	1.75 mm	68.76 KN	2.41 mm	97.21 KN	135.5J	15.3 J/g

	Energy Absorbed per Volume (MJ/m^3)
Single Porous NiTi Rod	$68.3MJ/m^3$
Composite Structure	$141.5MJ/m^3$
Al Foam	$20.0MJ/m^3$

Model for Composite Design

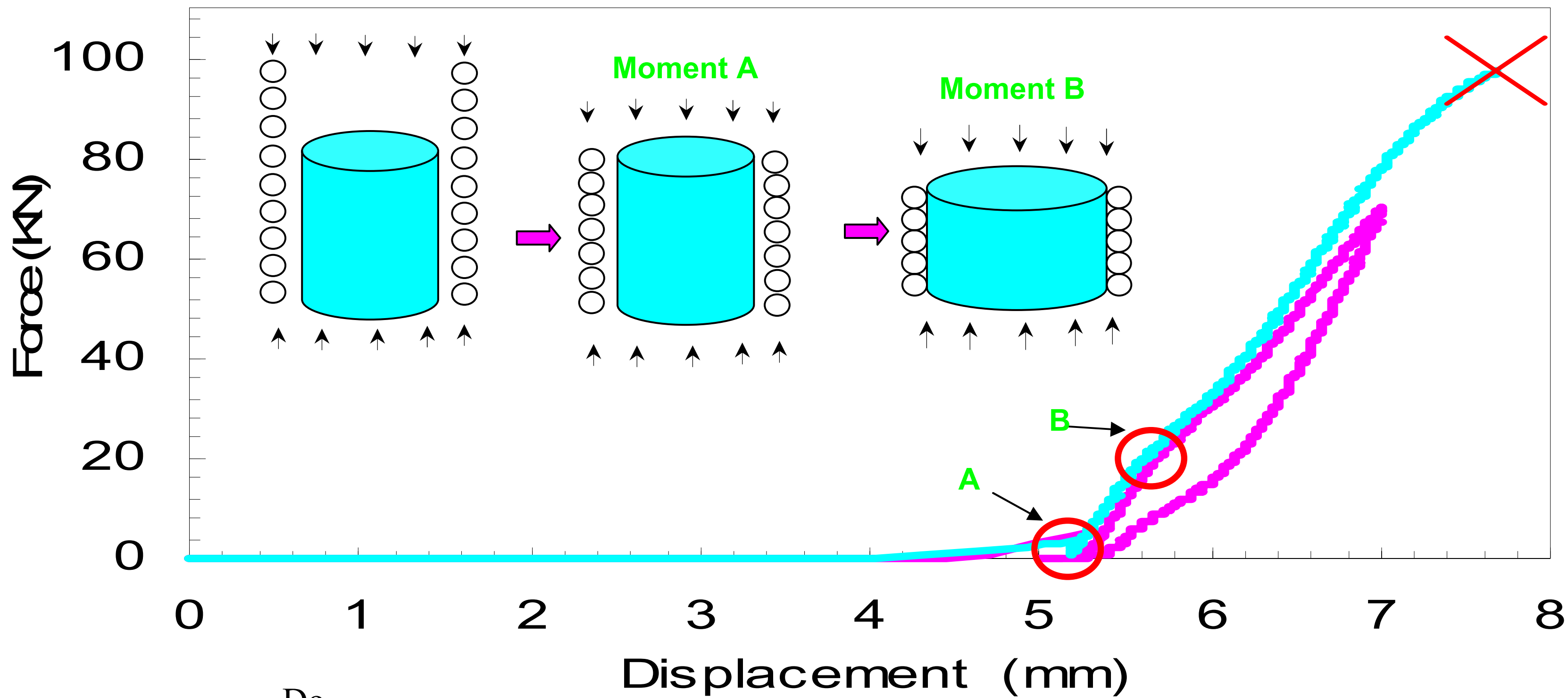

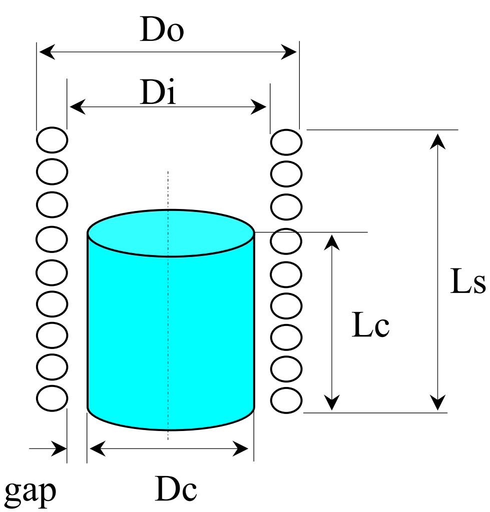

Ls = 20.3mm
Do = 12.4mm
Di = 9.1mm
Lc = 15.0mm
Dc = 9.0mm
gap = 0.05mm
Δh = 5.3mm

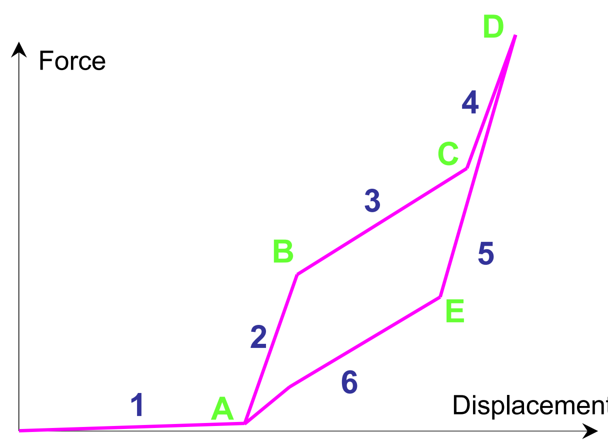

Force-Displacement relation after porous NiTi touches the NiTi spring

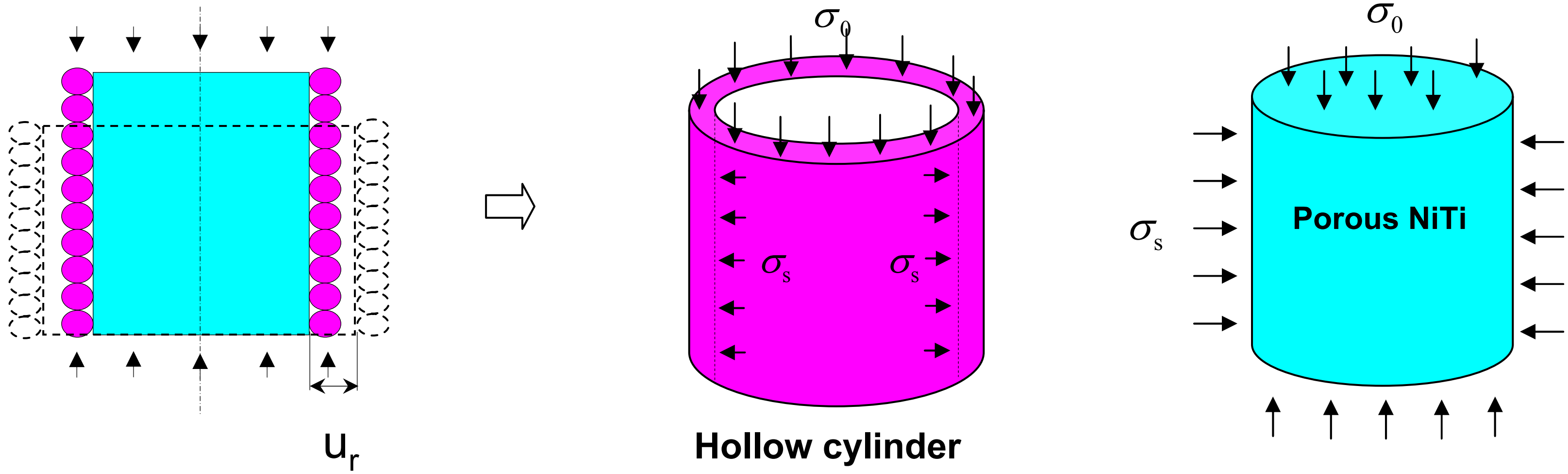

Substitute the strain-displacement relation into the stress-strain relation and then substitute into the equilibrium equation

$$\frac{\partial^2 u}{\partial r^2} + \frac{1}{r}\frac{\partial u}{\partial r} - \frac{u}{r^2} = 0 \quad \Longrightarrow \quad u_r = Ar$$

Boundary Condition - 1

Stress in the solid cylinder $\quad \sigma_r^c\left(r = \frac{D_c'}{2}\right) = \frac{E_c}{1-\nu^2}A + \frac{\nu}{1-\nu}\sigma_0 = \sigma_s$

Displacement in hollow cylinder at its inner surface

$$u_r^s = \frac{R_i}{E_s\left(R_o^2 - R_i^2\right)}\left\{\left[\left(1-2\nu\right)R_i^2 + \left(1+\nu\right)\right]\sigma_s + \nu\sigma_0 R_o^2\right\}$$

Displacement in solid cylinder at its surface

$$u_r^c = A\frac{D_c'}{2}$$

Boundary Condition - 2

The radial displacement of the solid cylinder and the inner surface of the hollow cylinder should be equal to keep the continuity of the whole structure

$$u_r^c = u_r^s$$

Solve the above equation for constant A

$$A = \frac{C_1 C_2 \frac{\nu}{1-\nu} + C_1 \nu R_o^2}{C_1 C_2 \frac{E_s}{1-\nu^2} + \frac{D_c'}{2}}$$

$$C_1 = \frac{R_i}{E_s\left(R_o^2 - R_i^2\right)}$$

$$C_2 = -\left[\left(1-2\nu^2\right)R_i^2 + \left(1+\nu\right)R_o^2\right]$$

Loading Curve

A: The spring shrinks to the same height as of the rod

$$F_A = \frac{G_s d^2}{64nR_o^2}\delta_A$$

B: The rod touches the spring

$$\delta_B = 0.45\text{mm}$$

$$F_B^c = 14\text{KN}$$

$$F_B^s = \pi\left(R_o^2 - R_i^2\right)E_s\delta_B / L_c$$

$$F_B = F_B^c + F_B^s$$

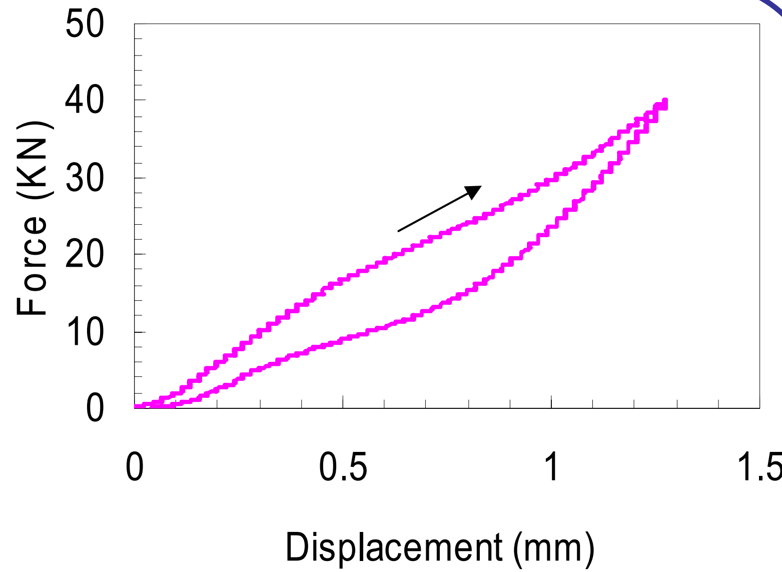

C: Finish martensite transformation

$$\delta_C = 0.92\text{mm}$$

$$F_C^c = \frac{\pi\left(\delta_C - \frac{2\nu}{1-\nu}Ah_C\right)E_T^c\left(D_C^c\right)^2}{4h_C\left(1-2\nu^2/(1-\nu)\right)}$$

$$F_C^s = \frac{\pi\left(\delta_C - \frac{2\nu}{1-\nu}Ah_C\right)E_s\left(R_o^2 - R_i^2\right)}{h_C\left(1-2\nu^2/(1-\nu)\right)}$$

$$F_C = F_C^c + F_C^s$$

D: Maximum reversible point

$$\delta_D = 1.75\text{mm}$$

$$F_D^c = \frac{\pi\left(\delta_D - \frac{2\nu}{1-\nu}Ah_D\right)E_M^c\left(D_D^c\right)^2}{4h_D\left(1-2\nu^2/(1-\nu)\right)}$$

$$F_D^s = \frac{\pi\left(\delta_D - \frac{2\nu}{1-\nu}Ah_D\right)E_s\left(R_o^2 - R_i^2\right)}{h_D\left(1-2\nu^2/(1-\nu)\right)}$$

$$F_D = F_D^c + F_D^s$$

Unloading Curve

E: Start austenite transformation

$$\delta_E = 0.90\text{mm}$$

$$F_E^c = \frac{\pi\left(\delta_E - \frac{2\nu}{1-\nu}Ah_E\right)E_M^c\left(D_E^c\right)^2}{4h_E\left(1-2\nu^2/(1-\nu)\right)}$$

$$F_E^s = \frac{\pi\left(\delta_E - \frac{2\nu}{1-\nu}Ah_E\right)E_s\left(R_o^2 - R_i^2\right)}{h_E\left(1-2\nu^2/(1-\nu)\right)}$$

$$F_E = F_E^c + F_E^s$$

F: Finish austenite transformation

$$\delta_F = 0.35\text{mm}$$

$$F_B^c = 7\text{KN}$$

$$F_F^s = \pi\left(R_o^2 - R_i^2\right)E_s\delta_F/L_c$$

$$F_F = F_F^c + F_F^s$$

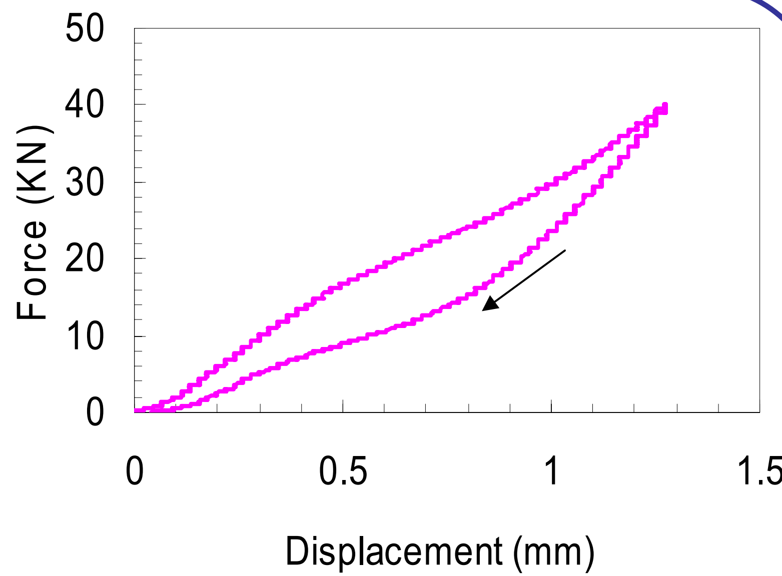

where

$$A = \frac{\left(C_1C_2\frac{\nu}{1-\nu} + \nu C_1R_o^2\right)\sigma_C^0}{C_1C_2\frac{E_M}{1-\nu^2} + \frac{D_B^c}{2}}$$

$$C_1 = \frac{R_i}{E_s\left(R_o^2 - R_i^2\right)}$$

$$C_2 = -\left[\left(1-2\nu^2\right)R_i^2 + (1+\nu)R_o^2\right]$$

Comparison of the predicted and experimental Force-Displacement curve

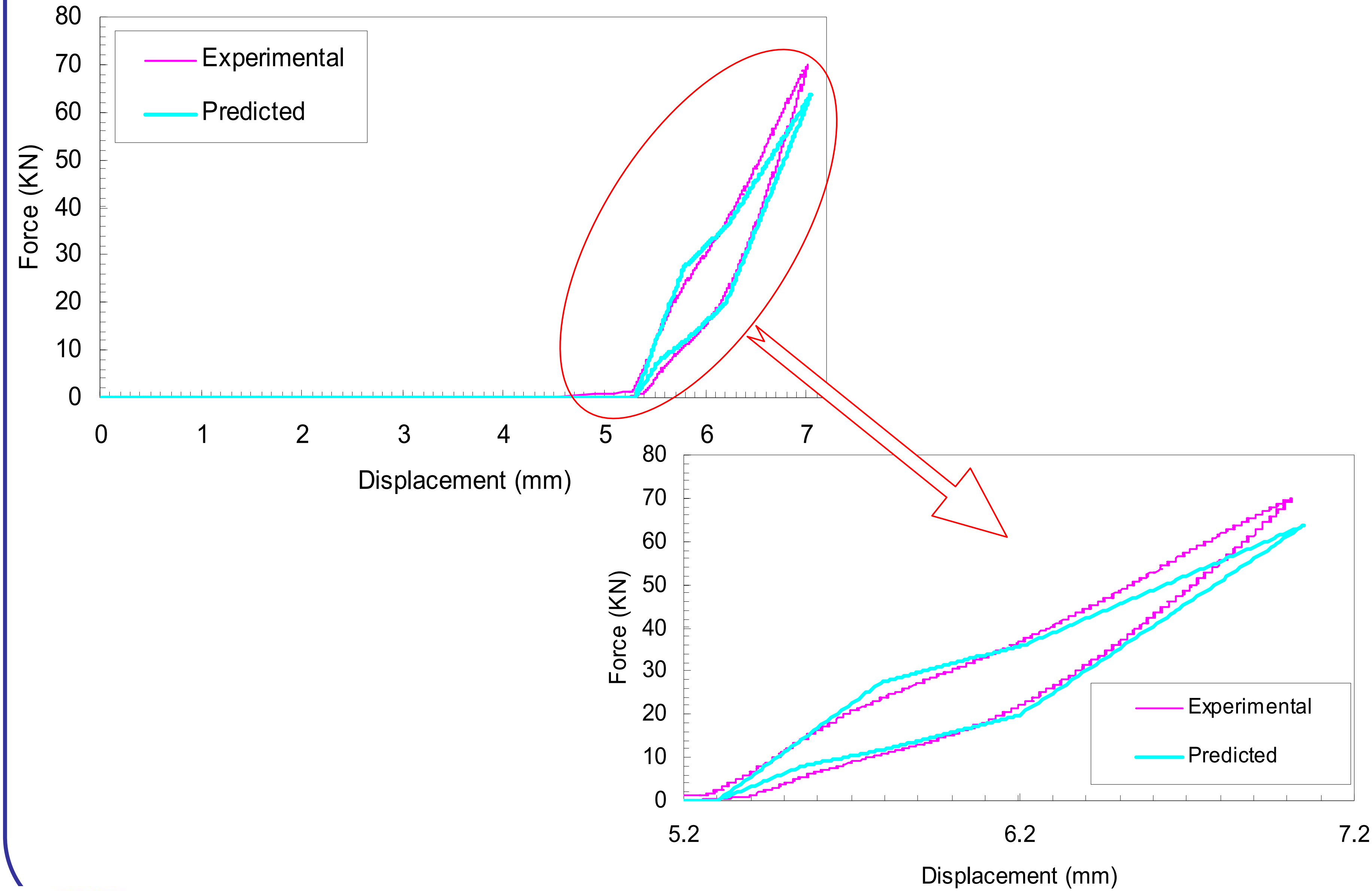

Conclusion

1. Successful processing ductile porous TiNi with high specific energy absorption capability by SPS

2. Establishment of analytical modeling of porous TiNi by micromechanic model

3. Design and demonstration of Composite made of concentric porous TiNi-SE and Spring of TiNi-SE grade